Report

Current Biology

The Nrde Pathway Mediates Small-RNA-Directed Histone H3 Lysine 27 Trimethylation in *Caenorhabditis elegans*

Graphical Abstract

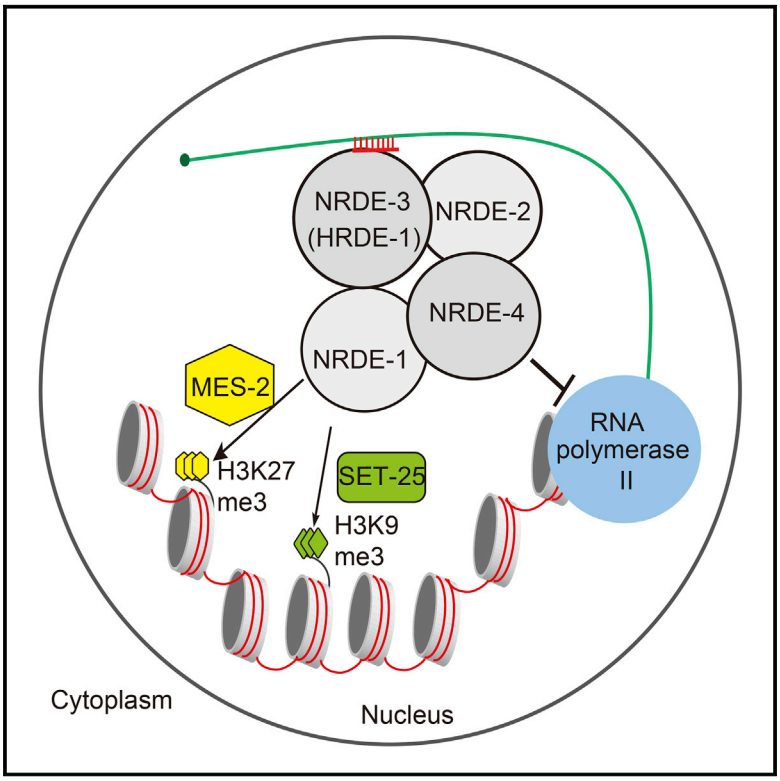

Authors

Hui Mao, Chengming Zhu, Dandan Zong, ..., Dun Liu, Xuezhu Feng, Shouhong Guang

Correspondence

fengxz@ustc.edu.cn (X.F.), sguang@ustc.edu.cn (S.G.)

In Brief

Mao et al. explore the relationship between small-RNA pathways and the acquisition and maintenance of the heterochromatic histone modification H3K27me3. This work reports that, in *C. elegans*, both exogenous and endogenous siRNAs can direct histone H3K27 methylation at targeted loci through the Nrde pathway.

Highlights

- Exo-RNAi induces H3K27me3 at targeted loci, a process depending on the Nrde pathway
- Endo-siRNA elicits H3K27me3 through the Nrde pathway
- Exo-RNAi-induced H3K27me3 is maintained for several generations
- RNAi-directed H3K9me3 and H3K27me3 have distinct genetic requirements

Mao et al., 2015, Current Biology *25*, 2398–2403
September 21, 2015
http://dx.doi.org/10.1016/j.cub.2015.07.051

CellPress

CellPress

Current Biology
Report

The Nrde Pathway Mediates Small-RNA-Directed Histone H3 Lysine 27 Trimethylation in *Caenorhabditis elegans*

Hui Mao,[1,2] Chengming Zhu,[1,2] Dandan Zong,[1] Chenchun Weng,[1] Xiangwei Yang,[1] Hui Huang,[1] Dun Liu,[1] Xuezhu Feng,[1,*] and Shouhong Guang[1,*]

[1]School of Life Sciences, University of Science and Technology of China, Hefei, Anhui 230027, China

[2]Co-first author

*Correspondence: fengxz@ustc.edu.cn (X.F.), sguang@ustc.edu.cn (S.G.)

http://dx.doi.org/10.1016/j.cub.2015.07.051

SUMMARY

Small-RNA-mediated chromatin modifications have been widely studied in plants and *S. pombe* [1–3]. However, direct evidence of small-RNA-guided sequence-specific chromatin alterations is scarce in animals [4–7]. In *C. elegans*, the nuclear RNAi defective (Nrde) pathway functions to transport siRNA from the cytoplasm to the nucleus, modulate transcription elongation, induce histone H3 lysine 9 (H3K9) trimethylation, and mediate transgenerational inheritance of RNAi [8–17]. Here, we show that both exogenous RNAi and NRDE-bound endogenous 22G RNAs can direct sequence-specific histone H3 lysine 27 (H3K27) trimethylation at targeted loci through the Nrde pathway. The resulting H3K27me3 status can be inherited by progeny for multiple generations. piRNAs and WAGO-1-associated siRNAs induce H3K27 methylation as well. Interestingly, CSR-1-associated endogenous siRNAs fail to trigger H3K27 methylation, whereas exogenous provision of dsRNAs can induce H3K27 methylation at the CSR-1-targeted loci via the Nrde pathway. We further observed distinct genetic requirements of H3K9 and H3K27 trimethylation. Whereas *set-25* and *met-2* are required for K9 methylation, *mes-2* is required for K27 methylation. The depletion of *mes-2* leads to a nuclear RNAi defective phenotype. These results indicate that dsRNA-triggered chromatin modification is a sequence-specific response that engages the Nrde pathway in *C. elegans*.

RESULTS

RNAi Can Direct Sequence-Specific Histone H3K27 Trimethylation

We previously conducted a genetic screen and identified the *nrde* factors specifically required for nuclear RNAi [8, 10]. Here, we tested a series of mutants that were reported to be defective in chromatin modifications [13, 15, 16] and found that *mes-2* is required for nuclear RNAi (Table S1). Similar to *eri-1*(*mg366*);*nrde-2*(*gg091*), the double mutant *eri-1*(*mg366*); *mes-2*(*bn11*) is defective in the silencing of *lir-1*, *lin-15b*, and *dpy-13* genes and modestly defective in *unc-15* silencing, although *pos-1* silencing is normal. MES-2 is a subunit of the Polycomb-like chromatin-repressive complex (PRC2), which acts as an H3 lysine 27 (H3K27) methyltransferase in *C. elegans* [18].

To investigate the relationship between Nrde pathway and H3K27 methylation, we first examined whether exogenously provided dsRNA can trigger H3K27 trimethylation by ChIP assay. We conducted the analysis in synchronized embryos, normalized the H3K27 methylation signal of the targeted site to that of *eft-3* gene, and calculated the relative H3K27me3 levels of animals with and without RNAi. Two independent antibody clones, Millipore nos. 07-449 and 17-662, were used to confirm that the results were consistent and specific to H3K27 methylation and not other histone modifications. dsRNAs targeting *lin-15b*, *lir-1*, or *dpy-28* induced a 2- to 5-fold enrichment of H3K27 methylation on the targeted genes in wild-type animals (Figures 1A, 1C, 1E, and S1A–S1C). We further evaluated the target specificity by comparing the levels of H3K27 methylation on *lin-15b*, *lir-1*, and *dpy-28* genes after *lin-15b* RNAi. dsRNA targeting *lin-15b* induced H3K27 methylation on *lin-15b*, but not on *lir-1* or *dpy-28* (Figures 1B and S1D). Similar specificity was observed when *lir-1* and *dpy-28* were RNAi silenced (Figures 1D, 1F, S1E, and S1F). Therefore, RNAi triggers sequence-specific H3K27 trimethylation.

eri-1(*mg366*) animals exhibit enhanced RNAi sensitivity compared with wild-type animals [19]. Correspondingly, dsRNA targeting *lin-15b* in *eri-1*(*mg366*) animals induced approximately 8-fold and 5-fold increases (detected with the no. 07-449 and no. 17-662 antibodies, respectively) of H3K27me3 on the *lin-15b* locus (Figures S1G and S1H).

As has been shown for dsRNA-induced H3 lysine 9 (H3K9) methylation [9, 12], the H3K27 methylation caused by RNAi can spread to nearby sequences. Whereas the dsRNA-targeted site exhibited the strongest increase in H3K27 trimethylation, sequences located adjacent to the targeted site in the genome also showed weak increases of H3K27me3 levels after RNAi (Figures 1A, 1C, 1E, and S1).

These data indicate that the H3K27 methylation induced by exogenous dsRNA is specific to the dsRNA-targeted gene and neighboring loci.

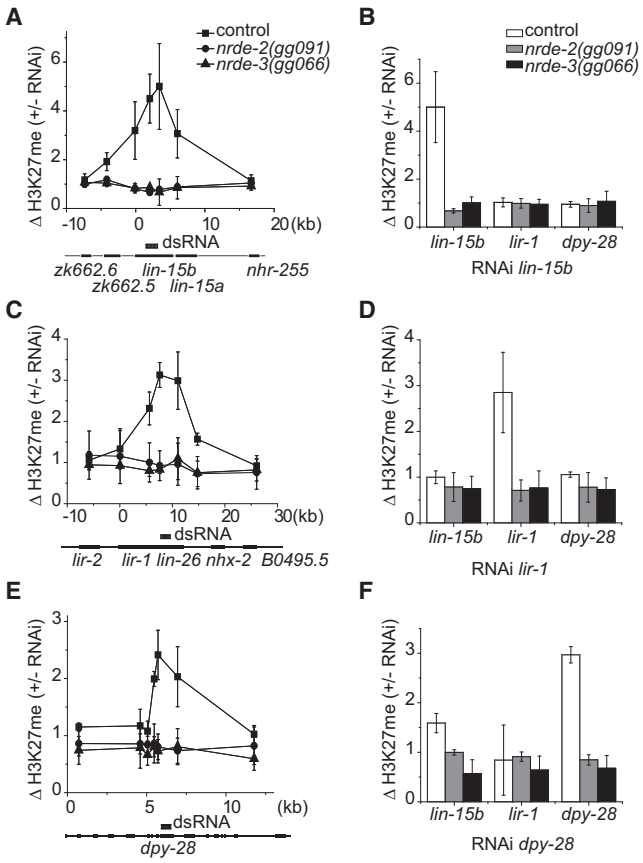

Figure 1. Nrde Pathway Is Required for Exogenous RNAi-Induced H3K27 Methylation

Animals of the indicated genotypes were exposed to dsRNA targeting *lin-15b* (A and B), *lir-1* (C and D), or *dpy-28* (E and F). H3K27 trimethylation levels of the targeted genes and their neighboring genes were measured by ChIP assay with anti-H3K27me3 antibody (Millipore no. 07-449) and quantified by real-time PCR. Multiple primer sets, which cover the whole gene body of the targeted genes, were applied for qPCR detection. Data are expressed as ratios of H3K27me3 in samples with RNAi to that of samples without RNAi. H3K27me3 signals from *eft-3* were used as an internal control for ChIP normalization. (n = 3 ± SD). See also Figure S1.

Nuclear RNAi Is Required for H3K27 Trimethylation

Next, we investigated the role of the Nrde pathway in small-RNA-induced H3K27 trimethylation. We found that dsRNA targeting *lin-15b*, *lir-1*, or *dpy-28* genes has little if any effect on the H3K27me3 status of the targeted loci in *nrde-2*(*gg091*) or *nrde-3*(*gg066*) animals (Figures 1A, 1C, and 1E). Similarly, small RNAs can elicit H3K9me3 through the Nrde pathway [9, 12]. Therefore, we conclude that the Nrde pathway is required for both H3K9 and H3K27 trimethylation induced by RNAi.

Nrde-Associated Endogenous siRNAs Direct H3K27 Trimethylation

The nuclear Argonaute protein NRDE-3 associates with a subset of 22G endo-siRNAs and directs H3K9 methylation in *C. elegans* [8]. We investigated whether NRDE-3-bound 22G siRNAs can elicit H3K27 methylation at targeted genomic loci.

e01g4.5 endo-siRNAs are among the most abundant endo-siRNAs expressed in *C. elegans* that bind to NRDE-3 [20]. A 6-fold decrease of H3K27me3 was observed in *e01g4.5* gene in both *nrde-2*(*gg091*) and *nrde-3*(*gg066*) mutants compared with wild-type N2 animals (Figure 2A). The nearby genes *e01g4.3* and *e01g4.6*, which express few endo-siRNAs, exhibit little change of H3K27 methylation levels in *nrde* mutants.

We assayed H3K27me3 levels in additional nuclear RNAi-targeted genes in *nrde-2*(*gg091*) and *nrde-3*(*gg066*) animals. Eight out of nine NRDE-3 targets exhibited decreased H3K27 methylation in both *nrde-2*(*gg091*) and *nrde-3*(*gg066*) mutants (Figure 2B). Nine out of 11 HRDE-1 targets exhibited decreased H3K27 methylation in *nrde-2*(*gg091*), but not *nrde-3*(*gg066*) animals. NRDE-3 and HRDE-1 are nuclear Argonautes expressed in the soma and germline, respectively [10, 21]. Both of these Argonaute proteins require NRDE-2 to conduct downstream nuclear RNAi processes [9]. The *dpy-28*, *ego-1*, *ama-1*, *lin-15b*, and *lir-1* genes, which express few NRDE-3 and HRDE1-associated endo-siRNAs [20], exhibit little NRDE-dependent H3K27 methylation (Figure 2B).

Therefore, we conclude that NRDE-3 and HRDE-1-bound endo-siRNAs direct H3K27 trimethylation in *C. elegans*.

piRNAs and WAGO-1-Associated 22G Endo-siRNAs Induce H3K27 Methylation

C. elegans expresses a number of classes of endogenous small RNAs, including microRNA, piRNA, and endo-siRNA. Here, we examined the H3K27 methylation on the sites targeted by various types of endogenous small RNAs.

piRNAs can direct the production of germline 22G siRNAs and mediate the transgenerational inheritance of gene silencing [13, 15, 16]. We observed a NRDE-2-dependent enrichment of H3K27me3 at piRNA targets (eight out of 14 genes; Figure S2A). WAGO-1 binds to a subset of germline 22G siRNAs. Three out of nine WAGO-1 targets showed a NRDE-2-dependent H3K27 methylation (Figure S2B).

To further investigate the target specificity of siRNA-induced H3K27me3, we analyzed the H3K27me3 levels of endogenous WAGO-1 targets during exo-RNAi. Wild-type and *nrde-2*(*gg091*) animals were both fed with or without *lin-15b* dsRNA, and the H3K27me3 levels of endogenous WAGO-1 targets were quantified (Figures S2C and S2D). We observed similar levels of H3K27me3 at the WAGO-1 targets in the presence or absence of *lin-15b* RNAi, which suggests exo-RNAi targeting *lin-15b* has little effect on H3K27 methylation of endogenous WAGO-1 targets.

CSR-1-Targeted Genomic Loci Can Be Methylated by Exo-RNAi through the Nrde Pathway

CSR-1 binds to endogenous 22G siRNAs and promotes germline gene expression [22–25]. We did not detect NRDE-dependent H3K27me3 marks at CSR-1-targeted sites (Figure S2E). Although these data do not exclude the possibility of CSR-1-dependent but NRDE-independent H3K27 methylation, we suspect that the means of biogenesis rather than the sequence of the siRNAs determine the effects of RNAi. Consistent with this idea, we found that three out of six CSR-1 target genes exhibited a NRDE-2-dependent increase of H3K27 methylation

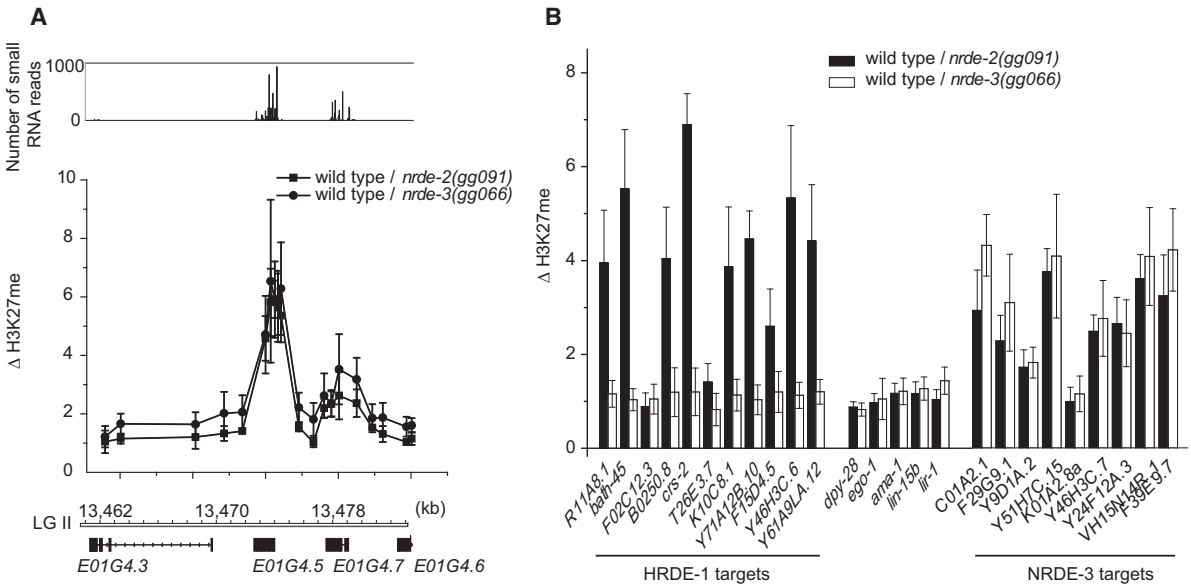

Figure 2. Nuclear RNAi-Associated Endo-siRNAs Direct H3K27 Methylation

H3K27me3 ChIPs were performed on wild-type, *nrde-2*(*gg091*), and *nrde-3*(*gg066*) animals. Data were presented as ratios of H3K27me3 in wild-type versus *nrde-2*(*gg091*) or wild-type versus *nrde-3*(*gg066*) animals. H3K27me3 signals from *eft-3* were used as an internal control for ChIP normalization (n = 3 ± SD). See also Figure S2.

(A) *e01g4.5* is an endo-siRNA target on chromosome II. The upper panel indicates NRDE-3-associated small RNAs, which were previously immunoprecipitated and deep sequenced [20]. The bottom panel indicates the level of H3K27me3.

(B) qRT-PCR quantification of DNA co-precipitating with H3K27me3 for additional nuclear RNAi targets. *dpy-28*, *ego-1*, *ama-1*, *lin-15b*, and *lir-1*, which express few NRDE-associated endo-siRNAs, did not exhibit H3K27me3 depletion in *nrde* mutants.

upon the exogenous provision of dsRNAs (Figure S2F). In addition, NRDE-2 associated with the pre-mRNA of the CSR-1 targets, but not with the control *eft-3* pre-mRNA, after exo-RNAi (Figure S2G).

dsRNAs Induce a Subgenic Chromatin Modification

To further investigate the relationship between the dsRNA trigger and the position of dsRNA-induced H3K27me3, we examined the effect of *lin-15b* triggers that target either the 5′ end or the 3′ end of the *lin-15b* gene (Figure S3A). We found that a 5-kb shift of the location of the triggers was accompanied by a corresponding shift in the H3K27 methylation peaks (Figures S3B and S3C). This spatial correlation between the triggering dsRNA and H3K27 methylation reveals that the specificity of the chromatin response is determined by events on a subgenic scale.

Transgenerational Inheritance of RNAi-Induced H3K27me3

dsRNA-triggered gene-silencing effects can last for multiple generations in *C. elegans,* but the ability to pass on those silencing effects is depending on both small-RNA-directed and chromatin-based mechanisms [21]. We observed that H3K27me3 can be inherited and maintained in the progeny of *oma-1*(RNAi) worms for multiple generations (Figure 3). Interestingly, the H3K27me3 marks eventually revert to the original state in the absence of the trigger. Our data suggest that H3K27me3 may play a role in the transgenerational inheritance of RNAi silencing.

Distinct Genetic Requirements for Small-RNA-Induced H3K9 and H3K27 Trimethylation

The mechanism underlying small-RNA-induced chromatin modifications is unclear in *C. elegans*. We investigated a series of mutants, which are implicated in chromatin binding and modifications, by H3K9me3 and H3K27me3 ChIP assays. We found that *set-25* and *met-2* are required for small-RNA-induced H3K9 methylation, similar to *nrde-3* (Figure 4A). The double mutant *set-25;met-2* exhibits H3K9me3 levels comparable to *set-25* or *met-2* single mutant, suggesting that they likely function in the same genetic pathway [26]. However, *set-25*, *set-32*, *hpl-1*, *hpl-2*, *met-1*, and *met-2* mutants failed to exhibit defects in small-RNA-induced H3K27 methylation (Figure 4B).

MES-2 is a homolog of *Drosophila* E(Z) and human EZH2. It contains a SET domain and functions as a histone methyltransferase [18]. Homozygous *mes-2* mutant is maternally sterile. We examined the H3K9 and H3K27 methylation levels following exo-RNAi against *lin-15b* and *mes-2* simultaneously. As controls, we performed double RNAi against *lin-15b* and *oma-1* as well as *lin-15b* and *nrde-2*. Double RNAi targeting *lin-15b* and *oma-1* together, but not *lin-15b* and *nrde-2*, induced an increase of both H3K9 and H3K27 methylation in *lin-15b* (Figures 4C and 4D). Strikingly, *mes-2* was only required for the RNAi-induced H3K27me3, but not for H3K9me3. MES-2, MES-3, and MES-6 are subunits of the PRC2 complex. We investigated the roles of MES-3 and -6 in nuclear RNAi (Figure S4A). We found that MES-6 was required for RNAi-induced H3K27me3. However, MES-3 likely prohibits small-RNA-induced H3K27me3,

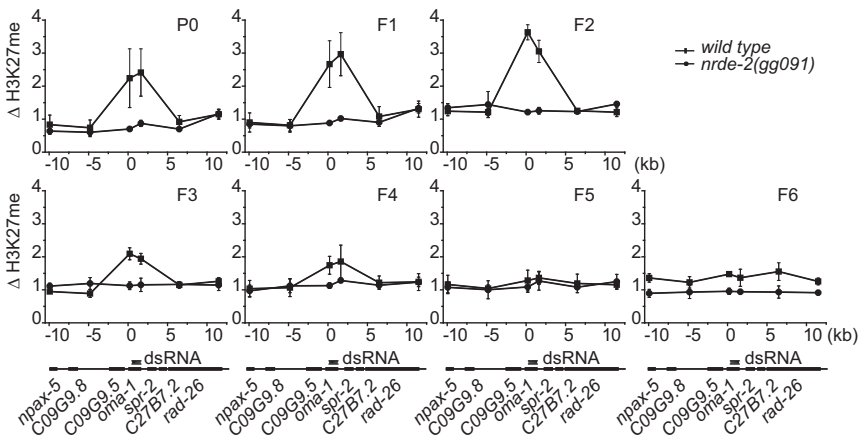

Figure 3. H3K27me3 Status Can Be Inherited for Multiple Generations

Wild-type and *nrde-2*(*gg091*) animals were exposed to *oma-1* dsRNA for two generations and then transferred to bacteria without RNAi. H3K27me3 levels were measured on synchronized young adults of each generation. Data were expressed as ratios of samples exposed to ± *oma-1* dsRNA (n = 3 ± SD). See also Figure S3.

suggesting that the subunits of PRC2 complex may have distinct roles in chromatin modifications. An H3K36 methyltransferase, MES-4, is required for the RNAi-induced H3K27me3 as well (Figure S4A). It has been shown that the PRC2 complex and MES-4 cooperate to promote the expression of germline genes and repress the X chromosomes and somatic genes [27]. Here, our data hint that MES-2/6 and MES-4 may also function together to mediate RNAi-induced H3K27me3, yet the mechanism is unclear.

In summary, these results suggest that the siRNA/NRDE complex can recruit different chromatin modification factors for H3K9 and H3K27 methylation.

H3K27 Methylation Is Required for Nuclear RNAi

We tested a series of *set* genes, which are putative histone methyltransferases, for possible roles in nuclear RNAi. Interestingly, mutants for *set-25*, a gene required for H3K9me3 and involved in transgenerational inheritance of RNAi [13, 15, 16], failed to exhibit pronounced nuclear RNAi defects (Table S1; Figures S4B–S4D). We speculate that H3K27 methylation is required for nuclear RNAi. Consistent with this idea, *mes-2* was required for RNAi targeting *lir-1*, *lin-15b*, and *dpy-13* (Table S1). *oma-1*(*zu405ts*) is a temperature-sensitive lethal allele of *oma-1* [28]. RNAi against *oma-1* suppressed *oma-1*(*zu405ts*) lethality; this suppression was partially blocked by *mes-2*(*bn11*) (Figure S4E). However, *mes-2* may also have Nrde-independent roles in RNAi. dsRNA-targeting *dpy-11* elicited a dumpy phenotype that can be suppressed by *rde-1* or *mes-2* mutation, but not by *nrde-2* or *nrde-3* mutation (Figures S4F and S4G).

Therefore, small-RNA-induced H3K27 trimethylation may play critical roles in nuclear RNAi.

DISCUSSION

Here, we show that the Nrde pathway is involved in small-RNA-directed H3K27 trimethylation in *C. elegans*. We describe several features of RNAi-induced H3K27me3 in *C. elegans*: (1) both exogenous and endogenous siRNAs are able to induce H3K27 methylation (Figures 1 and 2); (2) the chromatin modification is highly specific, with H3K27me3 triggered in a window surrounding the targeted genomic loci (Figure 1); (3) the H3K27me3 marks can be transmitted to progeny for multiple generations (Figure 3); and (4) H3K9 and H3K27 trimethylations have distinct genetic requirements, which may play different roles in nuclear RNAi (Figure 4; Table S1).

Several lines of evidence cumulatively suggest that H3K27me3 plays important roles in small-RNA-induced gene silencing. First, MES-2 is required for nuclear RNAi. *C. elegans* expresses approximately 38 SET-domain-containing proteins [29], yet MES-2 is the only known H3K27 methyltransferase. Second, *mes-2* is maternal sterile, whereas *nrde-2* progressively loses progeny [21]. Third, the Nrde pathway is involved in transgenerational inheritance of RNAi [21] and the PRC2 complex has also been shown to epigenetically transmit the memory of gene repression marks [30].

Interestingly, our data indicate that the Nrde pathway is a critical player in small-RNA-induced chromatin modifications in *C. elegans*. Both piRNAs and WAGO-1-bound 22G RNAs can induce NRDE-2-dependent H3K27 methylation (Figure S2). Consistently, piRNAs have been shown to elicit transgenerational gene silencing by inducing secondary 22G-RNA synthesis and utilize these siRNAs and NRDE-2 to mediate gene silencing (Figure S2) [13, 15, 16]. WAGO-1 is a germline Argonaute protein that binds to a subset of 22G-RNAs [31]. There are approximately 27 Agos encoded in the worm genome [32]. It will be very interesting to investigate how many of those Agos use the Nrde pathway to mediate chromatin modifications.

We proposed a working model of nuclear RNAi in *C. elegans*. siRNAs guide nuclear Argonaute proteins NRDE-3 or HRDE-1 to their targeted pre-mRNAs and then recruit NRDE-2, NRDE-4, and NRDE-1 to the pre-mRNAs and corresponding genomic loci. The NRDE complex further recruits MES-2 for H3K27 methylation and SET-25 for H3K9 methylation at the targeted genomic loci via unknown mechanisms.

EXPERIMENTAL PROCEDURES

Strains

Bristol strain N2 was used as the standard wild-type strain. All strains, except *oma-1*(*zu405ts*), were incubated at 20°C. *oma-1*(*zu405ts*) is a temperature-sensitive lethal strain that was grown at 15°C [28]. The strains used included *eri-1*(*mg366*), *his-24*(*ok1024*), *hpl-1*(*tm1624*), *hpl-2*(*tm1489*), *mes-2*(*bn11*), *met-1*(*n4337*), *met-2*(*n4256*), *nrde-2*(*gg091*), *nrde-3*(*gg066*), *oma-1*(*zu405ts*), *rde-1*(*ne219*), *sir-2.1*(*ok434*), *set-11*(*ok1619*), *set-12*(*n4442*), *set-13*(*ok2697*), *set-15*(*ok3291*), *set-19*(*ok1813*), *set-20*(*ok2022*), *set-21*(*ok2320*), *set-21*(*ok2320*), *set-25*(*n5021*), and *set-32*(*ok1457*).

RNAi

RNAi experiments were conducted as previously described [33]. Images were collected using a Leica DM2500 microscope.

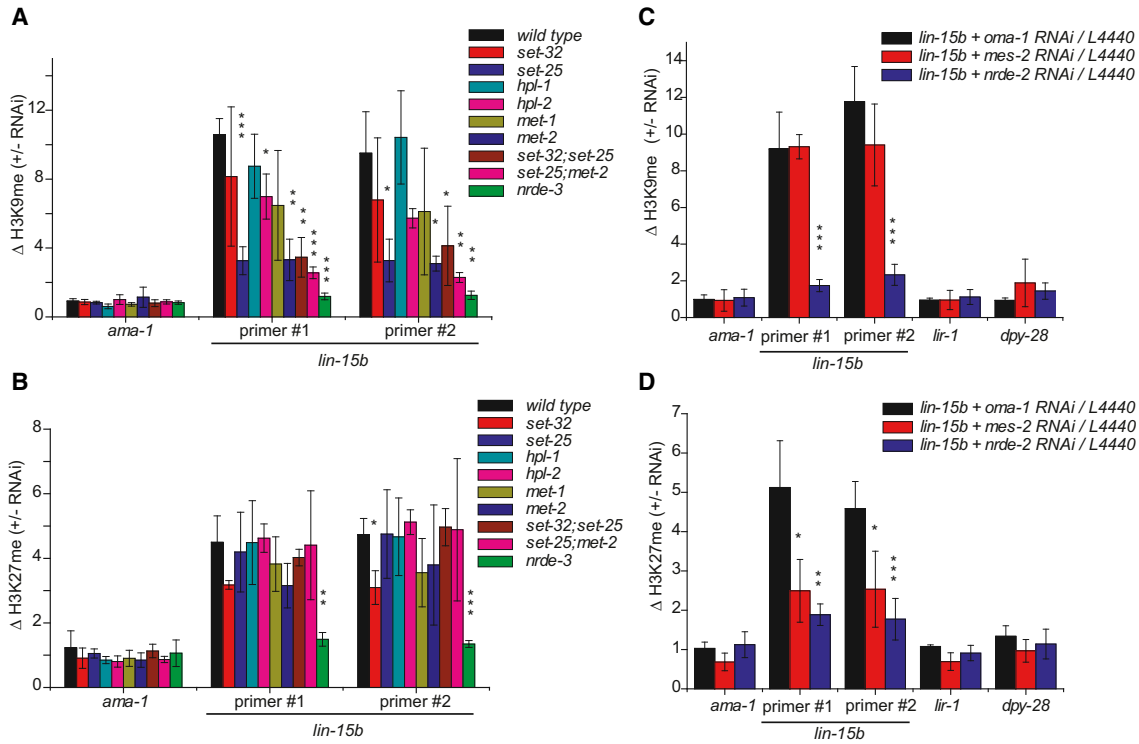

Figure 4. Distinct Genetic Requirements of Small-RNA-Induced H3K9 and H3K27 Trimethylation

(A and B) Animals of the indicated genotypes were exposed to *lin-15b* dsRNA or the empty vector control.

(C and D) Wild-type animals were exposed to dsRNAs targeting *1in-15b* and *oma-1*, *lin-15b* and *mes-2*, or *lin-15b* and *nrde-2*. ChIP assays were performed with H3K9me3 antibody (Millipore no. 07-523) or H3K27me3 antibody (Millipore no. 07-449) in synchronized embryos. Data were expressed as ratios of co-precipitating DNA in animals subjected to RNAi versus control animals (n = 3 ± SD). *eft-3* is used as an internal control, and *ama-1* is a negative control. Two primer sets were used for qRT-PCR. Student's t tests were applied.

*p < 0.05; **p < 0.01; ***p < 0.001. See also Figure S4.

Construction of dsRNA-Expressing Plasmids

HT115 bacteria expressing the empty vector L4440 (a gift from A. Fire) were used as controls. Bacteria expressing dsRNAs were mostly obtained from the Ahringer RNAi library and were sequenced to verify their identity [34]. *lin-15b* and *dpy-13* RNAi clones have been described previously [10, 20]. dsRNA targeting the 5′ end of *lin-15b* was PCR amplified with the primer pair 5′-gctaaagcttatgcaaacgctaaaaa and 5′-gctaaagcttcgtcctcatctccaaca from N2 genomic DNA, digested with HindIII and cloned into L4440. dsRNA targeting the 3′ end of *lin-15b* was PCR amplified with the primer pair 5′-gctaaagcttggc gaatatgttaaac and 5′-gctaaagctttcactcttccagcaat and inserted into the L4440 HindIII site. dsRNA-targeting *mes-2* was PCR amplified with the primers 5′-cccaagcttaatttgcctcgctttgtgaaaa and 5′-cccaagcttagcacggcatagtttgtagagt and inserted into the L4440 HindIII site. dsRNA-targeting *oma-1* was PCR amplified with the primers 5′-ggactagtccgaatgcagaaaccagaat and 5′-ggac tagtggccaagtttctatgggaca and inserted into the L4440 *Spe*I site.

ChIP

Chromatin immunoprecipitation (ChIP) experiments were performed as previously described with hypochlorite-isolated embryos or young adults [9]. After crosslinking, samples were resuspended in 1 ml FA buffer (50 mM Tris/HCl [pH 7.5], 1 mM EDTA, 1% Triton X-100, 0.1% sodium deoxycholate, and 150 mM NaCl) with proteinase inhibitor tablet (Roche no. 04693116001) and sonicated 23 cycles for embryos or 15 cycles for young adults at medium output (each cycle: 30 s on and 30 s off) with a Bioruptor 200. Lysates were precleared and then immunoprecipitated with 2 μl anti-trimethylated H3K9 antibody (Millipore no. 07-523) or 2 μl anti-trimethylated H3K27 antibody (Millipore no. 07-449 or Millipore no. 17-662). ChIP data of the targeted genes were normalized to co-immunoprecipitated *eft-3* promoter DNA. In exo-RNAi experiments, we normalized the ChIP signals to *eft-3* and expressed the data as ratios of indicated animals exposed to ± dsRNA. In endo-RNAi experiments, ChIP signals were normalized to *eft-3* first and then expressed as fold changes relative to control genotypes. Unless specified, the antibody Millipore no. 07-449 was used in most H3K27me3 ChIP experiments. The results shown are representative of three independent experiments. (n = 3 ± SD).

Sequences of real-time PCR primers were listed in Table S2. For each primer set, usually one primer targets an exon region whereas the other one targets an intron.

RIP

RNA immunoprecipitation (RIP) experiments were performed as previously described with hypochlorite-isolated embryos [10]. In particular, 3×FLAG::GFP::NRDE-2 was immunoprecipitated with anti-FLAG M2 antibody (Sigma; no. A2220). NRDE-2-bound RNAs were purified with TRIzol reagent and quantified by real-time PCR.

SUPPLEMENTAL INFORMATION

Supplemental Information includes four figures and two tables and can be found with this article online at http://dx.doi.org/10.1016/j.cub.2015.07.051.

AUTHOR CONTRIBUTIONS

H.M. contributed Figures 1A, 1B, 1E, 1F, 2B, 4, S1, S2A–S2E, S3, S4A, and S4E. C.Z. generated Figures 1C, 1D, 2A, 3, S2F, and S2G. D.Z., X.Y., and H.M. contributed to Table S1. C.W. and H.M. contributed to Figures S4B–S4D. H.H. and D.L. contributed to Figures S4F and S4G. X.F. and S.G. designed the project and wrote the manuscript.

ACKNOWLEDGMENTS

We are grateful to Drs. Zhong Zhao and Yupeng Yang and members of the S.G. lab for their comments. We are grateful to the Caenorhabditis Genetics Center, the International *C. elegans* Gene Knockout Consortium, and the National Bioresource Project for providing the strains. This work was supported by grants from the National Natural Science Foundation of China (31171254 and 31371323), the Chinese 973 Program (2011CBA01100), the Fundamental Research Funds for Central Universities (WK2060190018 and WK2070000034), and an intramural grant of the Chinese Academy of Sciences (KJZD-EW-L01-2).

Received: March 26, 2015
Revised: June 13, 2015
Accepted: July 20, 2015
Published: September 10, 2015

REFERENCES

1. Baulcombe, D. (2004). RNA silencing in plants. Nature *431*, 356–363.
2. Castel, S.E., and Martienssen, R.A. (2013). RNA interference in the nucleus: roles for small RNAs in transcription, epigenetics and beyond. Nat. Rev. Genet. *14*, 100–112.
3. Moazed, D. (2009). Small RNAs in transcriptional gene silencing and genome defence. Nature *457*, 413–420.
4. Kim, D.H., Villeneuve, L.M., Morris, K.V., and Rossi, J.J. (2006). Argonaute-1 directs siRNA-mediated transcriptional gene silencing in human cells. Nat. Struct. Mol. Biol. *13*, 793–797.
5. Kim, D.H., Saetrom, P., Snøve, O., Jr., and Rossi, J.J. (2008). MicroRNA-directed transcriptional gene silencing in mammalian cells. Proc. Natl. Acad. Sci. USA *105*, 16230–16235.
6. Cho, S., Park, J.S., and Kang, Y.K. (2014). AGO2 and SETDB1 cooperate in promoter-targeted transcriptional silencing of the androgen receptor gene. Nucleic Acids Res. *42*, 13545–13556.
7. Kanellopoulou, C., Muljo, S.A., Kung, A.L., Ganesan, S., Drapkin, R., Jenuwein, T., Livingston, D.M., and Rajewsky, K. (2005). Dicer-deficient mouse embryonic stem cells are defective in differentiation and centromeric silencing. Genes Dev. *19*, 489–501.
8. Burkhart, K.B., Guang, S., Buckley, B.A., Wong, L., Bochner, A.F., and Kennedy, S. (2011). A pre-mRNA-associating factor links endogenous siRNAs to chromatin regulation. PLoS Genet. *7*, e1002249.
9. Guang, S., Bochner, A.F., Burkhart, K.B., Burton, N., Pavelec, D.M., and Kennedy, S. (2010). Small regulatory RNAs inhibit RNA polymerase II during the elongation phase of transcription. Nature *465*, 1097–1101.
10. Guang, S., Bochner, A.F., Pavelec, D.M., Burkhart, K.B., Harding, S., Lachowiec, J., and Kennedy, S. (2008). An Argonaute transports siRNAs from the cytoplasm to the nucleus. Science *321*, 537–541.
11. Feng, X., and Guang, S. (2013). Small RNAs, RNAi and the inheritance of gene silencing in *Caenorhabditis elegans*. J. Genet. Genomics *40*, 153–160.
12. Gu, S.G., Pak, J., Guang, S., Maniar, J.M., Kennedy, S., and Fire, A. (2012). Amplification of siRNA in *Caenorhabditis elegans* generates a transgenerational sequence-targeted histone H3 lysine 9 methylation footprint. Nat. Genet. *44*, 157–164.
13. Ashe, A., Sapetschnig, A., Weick, E.M., Mitchell, J., Bagijn, M.P., Cording, A.C., Doebley, A.L., Goldstein, L.D., Lehrbach, N.J., Le Pen, J., et al. (2012). piRNAs can trigger a multigenerational epigenetic memory in the germline of *C. elegans*. Cell *150*, 88–99.
14. Conine, C.C., Moresco, J.J., Gu, W., Shirayama, M., Conte, D., Jr., Yates, J.R., 3rd, and Mello, C.C. (2013). Argonautes promote male fertility and provide a paternal memory of germline gene expression in *C. elegans*. Cell *155*, 1532–1544.
15. Shirayama, M., Seth, M., Lee, H.C., Gu, W., Ishidate, T., Conte, D., Jr., and Mello, C.C. (2012). piRNAs initiate an epigenetic memory of nonself RNA in the *C. elegans* germline. Cell *150*, 65–77.
16. Lee, H.C., Gu, W., Shirayama, M., Youngman, E., Conte, D., Jr., and Mello, C.C. (2012). *C. elegans* piRNAs mediate the genome-wide surveillance of germline transcripts. Cell *150*, 78–87.
17. Kelly, W.G. (2014). Transgenerational epigenetics in the germline cycle of *Caenorhabditis elegans*. Epigenetics Chromatin *7*, 6.
18. Bender, L.B., Cao, R., Zhang, Y., and Strome, S. (2004). The MES-2/MES-3/MES-6 complex and regulation of histone H3 methylation in *C. elegans*. Curr. Biol. *14*, 1639–1643.
19. Kennedy, S., Wang, D., and Ruvkun, G. (2004). A conserved siRNA-degrading RNase negatively regulates RNA interference in *C. elegans*. Nature *427*, 645–649.
20. Zhou, X., Xu, F., Mao, H., Ji, J., Yin, M., Feng, X., and Guang, S. (2014). Nuclear RNAi contributes to the silencing of off-target genes and repetitive sequences in *Caenorhabditis elegans*. Genetics *197*, 121–132.
21. Buckley, B.A., Burkhart, K.B., Gu, S.G., Spracklin, G., Kershner, A., Fritz, H., Kimble, J., Fire, A., and Kennedy, S. (2012). A nuclear Argonaute promotes multigenerational epigenetic inheritance and germline immortality. Nature *489*, 447–451.
22. Cecere, G., Hoersch, S., O'Keeffe, S., Sachidanandam, R., and Grishok, A. (2014). Global effects of the CSR-1 RNA interference pathway on the transcriptional landscape. Nat. Struct. Mol. Biol. *21*, 358–365.
23. Seth, M., Shirayama, M., Gu, W., Ishidate, T., Conte, D., Jr., and Mello, C.C. (2013). The *C. elegans* CSR-1 argonaute pathway counteracts epigenetic silencing to promote germline gene expression. Dev. Cell *27*, 656–663.
24. Tu, S., Wu, M.Z., Wang, J., Cutter, A.D., Weng, Z., and Claycomb, J.M. (2015). Comparative functional characterization of the CSR-1 22G-RNA pathway in *Caenorhabditis nematodes*. Nucleic Acids Res. *43*, 208–224.
25. Claycomb, J.M., Batista, P.J., Pang, K.M., Gu, W., Vasale, J.J., van Wolfswinkel, J.C., Chaves, D.A., Shirayama, M., Mitani, S., Ketting, R.F., et al. (2009). The Argonaute CSR-1 and its 22G-RNA cofactors are required for holocentric chromosome segregation. Cell *139*, 123–134.
26. Towbin, B.D., González-Aguilera, C., Sack, R., Gaidatzis, D., Kalck, V., Meister, P., Askjaer, P., and Gasser, S.M. (2012). Step-wise methylation of histone H3K9 positions heterochromatin at the nuclear periphery. Cell *150*, 934–947.
27. Gaydos, L.J., Rechtsteiner, A., Egelhofer, T.A., Carroll, C.R., and Strome, S. (2012). Antagonism between MES-4 and Polycomb repressive complex 2 promotes appropriate gene expression in *C. elegans* germ cells. Cell Rep. *2*, 1169–1177.
28. Detwiler, M.R., Reuben, M., Li, X., Rogers, E., and Lin, R. (2001). Two zinc finger proteins, OMA-1 and OMA-2, are redundantly required for oocyte maturation in *C. elegans*. Dev. Cell *1*, 187–199.
29. Andersen, E.C., and Horvitz, H.R. (2007). Two *C. elegans* histone methyltransferases repress lin-3 EGF transcription to inhibit vulval development. Development *134*, 2991–2999.
30. Gaydos, L.J., Wang, W., and Strome, S. (2014). Gene repression. H3K27me and PRC2 transmit a memory of repression across generations and during development. Science *345*, 1515–1518.
31. Gu, W., Shirayama, M., Conte, D., Jr., Vasale, J., Batista, P.J., Claycomb, J.M., Moresco, J.J., Youngman, E.M., Keys, J., Stoltz, M.J., et al. (2009). Distinct argonaute-mediated 22G-RNA pathways direct genome surveillance in the *C. elegans* germline. Mol. Cell *36*, 231–244.
32. Yigit, E., Batista, P.J., Bei, Y., Pang, K.M., Chen, C.C., Tolia, N.H., Joshua-Tor, L., Mitani, S., Simard, M.J., and Mello, C.C. (2006). Analysis of the *C. elegans* Argonaute family reveals that distinct Argonautes act sequentially during RNAi. Cell *127*, 747–757.
33. Timmons, L., Court, D.L., and Fire, A. (2001). Ingestion of bacterially expressed dsRNAs can produce specific and potent genetic interference in *Caenorhabditis elegans*. Gene *263*, 103–112.
34. Kamath, R.S., Fraser, A.G., Dong, Y., Poulin, G., Durbin, R., Gotta, M., Kanapin, A., Le Bot, N., Moreno, S., Sohrmann, M., et al. (2003). Systematic functional analysis of the *Caenorhabditis elegans* genome using RNAi. Nature *421*, 231–237.

